Journal of Food Engineering 89 (2008) 291–297

Contents lists available at ScienceDirect

Journal of Food Engineering

journal homepage: www.elsevier.com/locate/jfoodeng

An experimental machine vision system for sorting sweet tamarind

Bundit Jarimopas [a,*], Nitipong Jaisin [b]

[a] Department of Agricultural Engineering, Faculty of Engineering at Kamphaengsaen, Kasetsart University, Kamphaengsaen, Nakohnpathom, Thailand
[b] Program of Industrial Computer, Faculty of Industrial Technology, Chiangrai Rajbhut University, Chiangrai, Thailand

ARTICLE INFO

Article history:
Received 17 September 2007
Received in revised form 27 March 2008
Accepted 3 May 2008
Available online 15 May 2008

Keywords:
Sweet tamarind
Sorting
Image processing
Machine vision

ABSTRACT

The purpose of this research was to develop an efficient machine vision experimental sorting system for sweet tamarind pods based on image processing techniques. Relevant sorting parameters included shape (straight, slightly curved, and curved), size (small, medium, and large), and defects. The variables defining the shape and size of the sweet tamarind pods were shape index and pod length. A pod was said to have defects if it contained cracks.

The experiment involved the use of pods from two sweet tamarind cultivars: "Sitong" and "Srichompoo". The sorting system involved the use of a CCD camera which was adapted to work with a TV card, microcontrollers, sensors, and a microcomputer. Analysis was performed with image processing software. Analysis of variance was computed with regard to the variables of shape, size, and defects, and took into account variations in the control factors of belt speed, pod orientation, and spacing.

The results showed that the three control factors did not significantly affect shape, size, and defects at a significance level of 5%. The averaged shape indexes of the straight, slightly curved, and curved pods were 51.1%, 61.6%, and 75.8%, respectively. Pod length was found to be influenced by size and cultivar, with Sitong and Srichompoo pods ranging from 10.0 to 14.0 cm and 8.5 to 12.4 cm, respectively. The vision sorting system could separate Sitong tamarind pods at an average sorting efficiency (E_w) of 89.8%, with a mean contamination ratio ($\bar{C}_R$) of 10.2% at a capacity of 1517 pod/h. Respective figures for Srichompoo pods were E_w; 94.3%; $\bar{C}_R$, 5.7%; and capacity, 1491 pod/h. The contamination ratios met the export standards mandated by the Thai agricultural commodities and food codification.

1. Introduction

Sweet tamarind (*Tamarindus indica L.*) is one of the most popular fruit varieties in Thailand. The fruit, which is actually a pod, is harvested ripe and consumed fresh. Sweet tamarind has low water content and is high in phosphorus, potassium, thiamin, and niacine (Gunasena and Hughes, 2000). The two most popular cultivars are known locally as "Sitong" and "Srichompoo".

Fig. 1 depicts the three typical shapes of sweet tamarind pods: straight, slightly curved, and curved. (Sitong pods typically are more curved than Srichompoo pods.) A damaged pod is also displayed. Increases in pod curving are attributed by growers to rain shortages and sharp drop in air temperature.

The sweet tamarind pod comprises a shell and flesh, within which are enclosed seeds. The shell clearly separates from the flesh as the pod approaches maturity. Sitong shells are appreciably more rippled and have a higher flute than the Srichompoo variety. As the shells of both varieties are quite dry (moisture content is about 18.6% (Jarimopas et al., in press)), and have no direct interior support, they are prone to breakage when subjected to mechanical loading.

One of the most important operations in a packing line is sorting (including sizing). Such an operation requires several parameters to be quickly identified and managed at the same time. These include variety, maturity, color, shape, size, and defects. The efficiency and effectiveness of the sorting govern the quality standard of the packing lines and product (Office of Thai Agricultural Commodity and Food Standard, 2003), which in turn determines the marketability of the product. Accordingly, there is need for a robust, consistent, rapid, and cost effective sorting method.

Manual sorting continues to be the most prevalent method used. Problems inherent in this system include high labor costs, worker fatigue, inconsistency, variability, and scarcity of trained labor. The paucity of available labor and increasing employment costs during the peak harvesting seasons have been identified as the important factors driving the demand for automation of the industry.

One of the most practical and successful techniques for nondestructive quality evaluation and sorting of agricultural products is the electro-optical technique, which judges the optical properties of the product (Chen, 1996). This technique – which can be used to detect color uniformity, shape, size, external defects, foreign

* Corresponding author. Tel.: +66 34 281099; fax: +66 34 351842.
E-mail address: jarimopas@yahoo.com (B. Jarimopas).

0260-8774/$ - see front matter © 2008 Elsevier Ltd. All rights reserved.
doi:10.1016/j.jfoodeng.2008.05.007

materials, and disease – has been used for post-harvest grading for a wide variety of agricultural products. According to Jayas and Karunakaran (2005), a machine vision system is a nondestructive, objective, rapid, and cost effective technique that determines the external and internal characteristics of products, including maturity, ripeness, bruises, defects, moisture, and nutrients. They say the method not only identifies the presence of defects but also can be used to quantify defects so that only those products which meet minimum grading requirements will be sorted for consumption. For these reasons the visible spectrum system measuring reflectance properties are the most widely adopted forms of technology in the industry.

The visible-wavelength cameras comprising charge coupled devices (CCDs) used in this experiment assessed the monochrome and colour grades of area-scans or line-scans to determine the reflectance characteristics of products illuminated by a light source. This technique is explained by Ruenfaikas (2005), who states that objects of a desired color can be distinguished from a background after separating each pixel in an image into the primary RGB colors. A practical application has been demonstrated by Blasco et al. (2003), who developed a machine vision system to automatically grade apples according to size, color, stem, and external blemishes. A segmentation procedure based on Bayesian discriminant analysis was used to distinguish the fruit, stem, and blemishes from the background resulting in precise grading (repeatability tests for blemish detection and size estimation returned results of 86% and 93%, respectively).

In another example, Pearson and Slaughter (1996) applied line-scans from computer vision to detect early split lesions in the hulls of pistachio nuts. Gray scale intensity profiles were computed across the width of the nut, and profiles crossing an early split lesion – illustrated by a deep and narrow valley on the profile – were computed every 0.5 mm along the longitudinal axis of the nut. The numbers of adjacent profiles with deep and narrow valleys were recorded and it was determined that nuts with early split lesions contained a significantly higher count of these adjacent profiles than normal nuts. All the early split nuts and 99% of the normal nuts were correctly classified in this fashion.

A final illustration is to be found by Li et al. (2002). They developed computer image technology for apple surface defect detection which allows graders to remove image background, to identify the stem-end and calyx areas, and to ascertain segment defects. The detection hardware features two CCD monochromatic cameras mounted above and below a conveyor in a lighting chamber and two mirrors fixed on both sides of the conveyor, which provided four simultaneous images of the scanned fruit. The background is removed by the subtracting method and defects are extracted by comparing the scanned fruit with normalized reference apple images. Testing of the single row computer image sorting system indicated 93% classification accuracy.

Like apples and pistachio nuts, sweet tamarind for much of history has been manually sorted. The examples described above show that it has been possible to automatically sort the first two mentioned agricultural products; accordingly, the objective of this

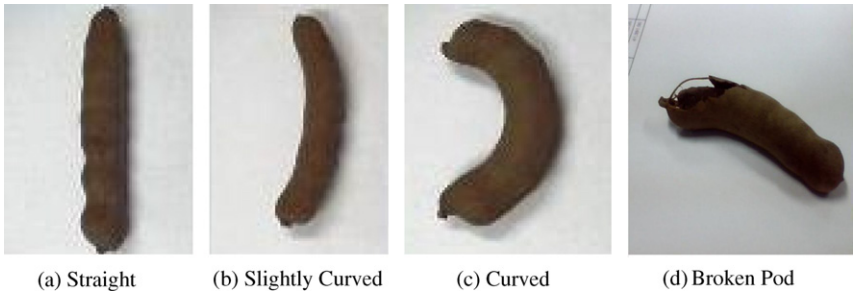

Fig. 1. Various appearances of sweet tamarind. (a) Straight, (b) slightly curved, (c) curved, and (d) broken pod.

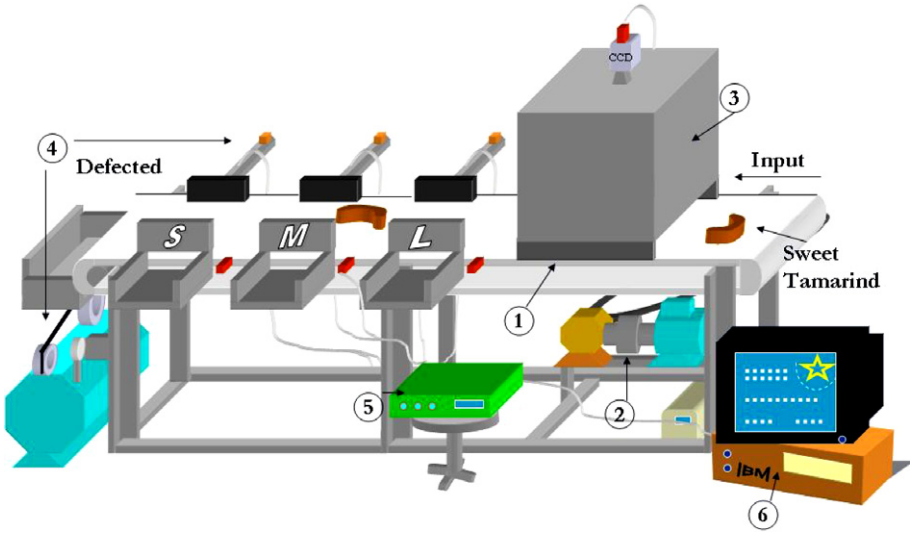

Fig. 2. An experimental machine vision system for sorting sweet tamarind pods (1 is conveyor; 2 is power drive; 3 is light source and CCD camera; 4 is pneumatic segregator and compressed air tank; 5 is control unit; and 6 is microcomputer).

research was to develop an efficient automated sorting system for sweet tamarind pods based on the image processing techniques that have been effectively used with apples and pistachios.

2. Materials and methods

2.1. Hardware and software design

The hardware included a conveyor, power drive, light source and image sensor, pneumatic segregator, control unit, and microcomputer. The software consisted of systems for shape sorting, sizing, and defect detection.

2.1.1. Hardware

Fig. 2 shows the experimental sweet tamarind sorting system. It featured a 30 cm wide and 180 cm long white conveyor belt with four receivers for the sorted sweet tamarind. The conveyor was driven by a 375-watt, three-phase ABB electric motor with a 1:80 ABB gear reducer. On the right side of the belt was a box with a CCD camera mounted on the top and four 14-watt energy saving lamps at each corner of the box to give uniform light intensity with minimum shadows. The camera, which was mounted about 41 cm above the belt, had a focal length of 38–72 mm and provided a resolution of 520 vertical TV lines. A cylinder of compressed air was used to drive the three pneumatic segregators. The sorting system was so designed as to sort sweet tamarind into three sizes (large, medium, and small). The defective pods were rejected at the left hand end of the conveyor. The electronic control unit (Fig. 3) comprised a master microcontroller (AT 89 S 8252), a slave microcontroller (AT 89 C 2051), and a signal conditioner. The signal conditioner featured a comparator (Op-amp TLC 272) to regulate the signal level of the photosensor to the master microcontroller. The control unit components were assembled in a box and placed under the sorting system. The microcomputer (microprocessor speed: 1.6 GHz) was used for signal processing and was equipped with frame grabber card (25 fps).

2.1.2. Operation

Sweet tamarind pods were fed into the sorting system from the right side of the belt conveyor. While travelling on the conveyor, the pod passed a photosensor comprising a laser diode and phototransistor. The signal produced by the sensor was sent to the master microcontroller, where it was processed and sent onwards through a serial port to the frame grabber in the microcomputer. The frame grabber commanded the CCD camera to take an image and then returned the image signal to the grabber for processing into a digital signal. Next, the digital image signal was sent to the microcomputer for analyses of size, shape, and defects. The results were sent back to the master microcontroller, where they were converted into commands or codes representing various grades; these commands and codes were then sent to the slave microcontroller. The slave compared the signal produced by the sensors at the S, M and L stations with the predetermined grades to ascertain whether any of the signals pertained to any of the predetermined grades. If a match occurred, the slave continued repeatedly sent commands to the solenoid valve of the chosen station until its shaft was actuated and the sweet tamarind pod was pushed from the belt into the receiver.

2.1.3. Software

2.1.3.1. Image pre-processing. A computer program, written in Borland C++5.0, was developed to process and analyze the images. The computer program was written with applications that pertained specifically to the functions of sorting shapes, sizes, and defects. It contained an image pre-processing routine which standardized images by means of an 8 bit/pixel histogram that eliminated noise and expanded the image. The histogram coordinate was (X, Y), where X refers to position and Y refers to light intensity ranging from 0 (black) to 255 (white). Y could be estimated from

$$Y = 0.299R + 0.587G + 0.114B \tag{1}$$

where R, G, and B were obtained from the real color image. The pre-processed image was further segmented to separate the object from its background by the use of threshold (T^t). The threshold value was calculated from the following equation (Sonka et al., 1998):

$$\mu_o^t = \frac{\sum(x,y) \in \text{objects } f(x,y)}{\#\text{object\_pixels}} \tag{2}$$

$$\mu_B^t = \frac{\sum(x,y) \in \text{background } f(x,y)}{\#\text{background\_pixels}} \tag{3}$$

$$T^{(t+1)} = \frac{1}{2}\left(\mu_B^t + \mu_o^t\right) \tag{4}$$

where μ_o^t is the average intensity of object; μ_B^t is the average intensity of background; objects $f(x, y)$ is the object intensity which was less than T^t; #objects_pixels is the number of pixels having an object intensity less than T^t; background $f(x, y)$ is the background intensity which was more than T^t; #background_pixels is the number of pixels having background intensity more than T^t; $T^{(t)}$ is the threshold value of intensity on grey scale at time t; and $T^{(t+1)}$ is the threshold value of intensity on grey scale at time t+1.

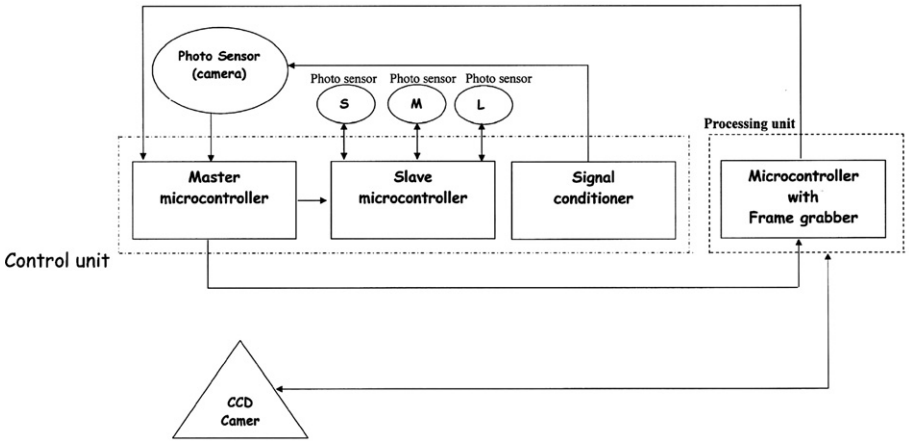

Fig. 3. Block diagram depicting functional units.

The new $T^{(t)}$ was repeatedly tested by Eq. (4) until $T^{(t+1)} = T^{(t)}$ was obtained, resulting in the required threshold separation of background and object. The original color picture of the sweet tamarind was calibrated through the use of Eqs. (1)–(4) until the black and white picture represented in Fig. 4 was produced.

2.1.3.2. Determination of shape. The shape of the sweet tamarind pod could be identified from its curvature. The shape was categorized into "curved", "slightly curved", and "straight". The Sitong pod typically is curved while the Srichompoo pod is normally straight. Slightly curved pods are found in both cultivars. In order to find the shape index of a sweet tamarind pod, the center of the image was first located (Fig. 4). Coordinates of the image center could be determined from the following equations (Ruenfaikas, 2005):

$$X_C = \sum \frac{X_i}{N} \tag{5}$$

$$Y_C = \sum \frac{Y_i}{N} \tag{6}$$

where i is the order of black pixels; N is the number of black pixels; X_i and Y_i are the position of black pixels along X and Y axes; and X_C and Y_C are the position of the image centers along X and Y axes.

A circle of 55 pixel radius (which is bigger than the radius of ordinary sweet tamarind pods) was made to encircle the image of the sweet tamarind. A point of 0° was located on the circumference and a radial line was drawn toward the image center (X_C, Y_C) until the line (r_i) reached a black pixel. The value of r_i for each degree, i, along the circumference in a counterclockwise direction was determined for the entire 360°. The length of r_i was plotted on the graph with respect to the scanning degree in Fig. 5. The difference in r_i of Fig. 5 (called Δ) at the points i and i+1 was repeatedly determined for the whole graph and used to create the graph in Fig. 6. This graph was used to determine the pulses indicating the position of the stem and tail of the sweet tamarind. The clearance along the scanning degree axis between the pulses of the stem and tail of the sweet tamarind (normalized to the 360° of a circle (shape index)) could be estimated from

$$C = 100 \times \frac{p - (\mathrm{sd}_{\max} - \mathrm{sd}_{\min})}{p} \tag{7}$$

where C is the shape index expressed by clearance in scanning degrees corresponding to $\mathrm{sd}_{\max}$ and $\mathrm{sd}_{\min}$ normalized to 360° (%); $\mathrm{sd}_{\max}$ is the scanning degree of stem pulse; $\mathrm{sd}_{\min}$ is the scanning degree of tail pulse; and p is the scanning degree of a circle (360). The above principle was applicable to the slightly curved and the straight pods.

2.1.3.3. Determination of size. Several researchers have used length as a sizing parameter for characterizing fruit size (Peleg, 1985; Jarimopas et al., 1999; Kawano, 1994). If this is accepted, let $H(H_x, H_y)$ and $T(T_x, T_y)$ be the points of coordinates of stem and tail of the sweet tamarind pod along x and y axes (Fig. 7) (the H and T were previously obtained as described in Section 2.1.3.2). The length of HT could then be determined from

$$HT = \sqrt{(H_x - T_x)^2 + (H_y - T_y)^2} \tag{8}$$

Scanning was conducted from Q in the middle of HT and perpendicular to HT to one side. Whenever a pixel changing from white to black was found, C was then located. Whenever the scanning was changed from black pixel to white pixel, D and Z_{11} – which was half of the distance CD – were located. Scanning would be repeated from Q to the opposite side if the black pixel was not found when scanning reached a pixel radius of 55. Radial scanning from Q to the sweet tamarind pod was made with an increment of 1° counterclockwise to QCD. The middle point of the sweet tamarind pod was located again at Z_{12}. Knowing the coordinates of Z_{11}

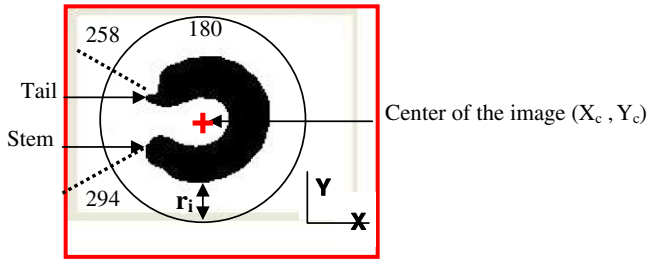

Fig. 4. Determination of the center and curvature of sweet tamarind pods (scanning degrees of the stem and tail pulse were 294 and 258, respectively).

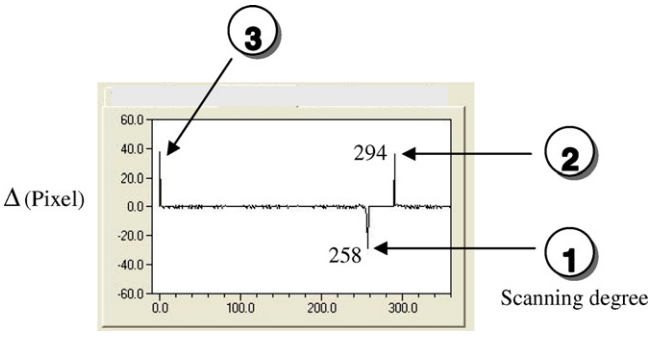

Fig. 6. Graph of pulse of sweet tamarind corresponding to stem and tail (1 is $\mathrm{sd}_{\min}$; 2 is $\mathrm{sd}_{\max}$; 3 is starting point; and $\Delta = r_{i+1} - r_i$).

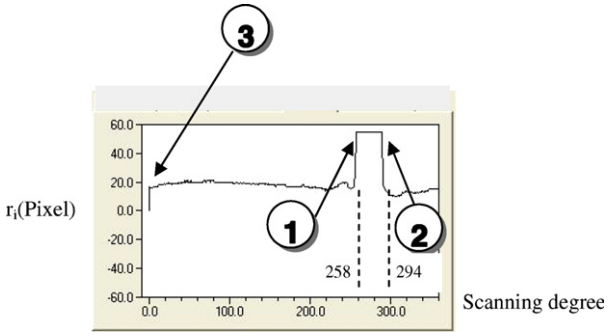

Fig. 5. Graph determining the curvature of sweet tamarind pods (1 is $\mathrm{sd}_{\min}$; 2 is $\mathrm{sd}_{\max}$; and 3 is starting point).

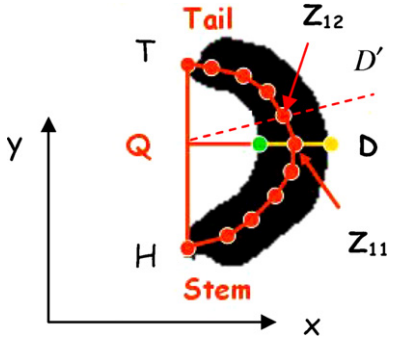

Fig. 7. Binary image for determining sweet tamarind pod length.

and Z_{12}, the increment distance from Z_{11} to Z_{12} could then be calculated. Similar scanning was repeated both counterclockwise and clockwise until the middle point of the sweet tamarind pod could not be located. The length, L, of the sweet tamarind pod could be estimated from the sum of the increment distances between the adjacent middle points from stem to tail points.

When point Q lies inside the black pixels area, it indicates that the tamarind pod is a straight pod. In this case, the length of the pod can be estimated by the distance HT.

2.1.3.4. Determination of defects. The main defects suffered by sweet tamarind pods are caused by breakage of the shell (Jarimopas and Sirisawas, 2006) in such a way that the broken piece of shell is missing, and the inside flesh is exposed. The color of the flesh typically is dark brown, which contrasts with the light brown or grey of the shell. Fig. 8 shows the grey scale of a defective sweet tamarind. From this, by using Eqs. (2) and (3), the image of white pod and black flesh was obtained. Grey color was further added to the pod to clearly distinguish the environment (in this case, the white conveyor belt) from the pod and flesh. The size of the defect could be quantified as follows:

$$\text{Defect percentage} = \frac{\text{Number of black pixels}}{\text{Number of black pixels} + \text{number of grey pixels}} \quad (9)$$

2.2. Performance test

2.2.1. Determination of proper height of CCD camera

Optics theory (Serway, 1996) suggests that optimum object distance can be derived from the given focal length of the camera and the desired image distance. In this experiment, the CCD camera was mounted on a metallic stand which had an adjustable height. A piece of 2 cm × 2 cm paper was placed on the platform under the camera and in the line of sight of the camera lens. In the first phase, the camera was mounted 35 cm above the paper. An image of the area was taken, processed and recorded on three separate occasions. This procedure was repeated for other combinations of camera height (37, 40, 44, 47, and 49 cm) and paper size (3, 4, 5, 7, and 9 cm). The percent error of system readings was calculated as follows: true dimension of the paper − ((read value/true dimension) × 100).

2.2.2. Influence of conveyor speed, spacing, and orientation of sweet tamarind pods on shape, size, and defect parameters

2.2.2.1. Shape. Thirty straight undamaged sweet tamarind pods of uniform size were selected at random. The first pod was placed on the white belt conveyor belt with its stem pointing to the left side of the sorting machine in parallel to the belt movement (corresponding to angular displacement = 0° with respect to the direction of belt movement). Belt speed was zero. An image of the pod was taken, processed, and recorded. The same procedure was repeated for the other seven θ (45, 90, 135, 180, 225, 270, and 315°). This procedure was repeated with the rest of the samples by continuously placing each straight pod 20 cm apart at $\theta = 0°$ on the belt conveyor, which was traveling at a speed of 10.28 m/min. Thirty replications were made for each combination of θ, belt speed (10.28, 13.34, and 17.47 m/min) and spacing (20, 25, and 30 cm). The experiment was repeated with the curved and the slightly curved sweet tamarind pods. ANOVA and Duncan multiple range test (DMRT) were applied for analysis.

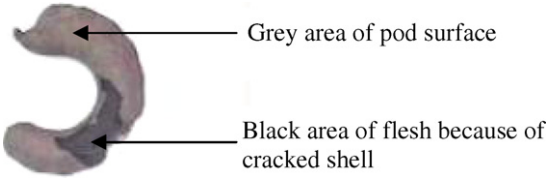

Fig. 8. Grey scale image of defective sweet tamarind pod.

2.2.2.2. Size. Thirty samples of undamaged Sitong pods of each of the three sizes (small, medium, and large) were selected randomly. The procedure described in the preceding paragraph was repeated. The same experiment was repeated with Srichompoo pods.

2.2.2.3. Defects. Circular holes measuring 2 mm were made in the center of selected pods to simulate the defect of pod breakage. Twenty "damaged" pods were placed on the moving belt at varying speeds (0, 10.28, 13.34, and 17.47 m/min) and spacings (20, 25, and 30 cm). An image of each pod was taken, processed, and recorded. The procedure was repeated with pods that contained differing hole-sizes (3, 4, 5, 6, 7, 10, and 13 mm in diameter). ANOVA and Duncan multiple range tests were applied for analysis. The percentage of detected defects was estimated as follows:

$$\text{Percent detected} = \frac{1 - (\text{True area} - \text{Read area})}{\text{True area}} \times 100 \quad (10)$$

2.2.3. Performance of the machine vision system

The sorting system was operated under conditions that were considered to be optimum with regard to belt speed, pod spacing, and pod orientation, as determined by the procedures described above. A total of 300 pods from the two cultivars – 50 pods from each of the three sizes within each cultivar – were randomly selected from the orchard. Size separation was calculated according to Eq. (11) (Peleg, 1985) and applied to the sorting system.

$$X_{s1} = \left[\frac{\mu_2\sigma_1^2 - \mu_1\sigma_2^2}{\sigma_1^2 - \sigma_2^2}\right] + \left[\left(\frac{\mu_2\sigma_1^2 - \mu_1\sigma_2^2}{\sigma_1^2 - \sigma_2^2}\right)^2 - \frac{\mu_2^2\sigma_1^2 - \mu_1^2\sigma_2^2 - 2\sigma_1^2\sigma_2^2\ln(\sigma_1/\sigma_2)}{\sigma_1^2 - \sigma_2^2}\right]^{1/2} \quad (11)$$

where X_{s1} is the optimum size between two adjacent size distributions; μ_1 and μ_2 are the means of size distribution numbers 1 and 2; σ_1 and σ_2 are the standard deviation related to μ_1 and μ_2; and σ_1^2 and σ_2^2 are the variance related to μ_1 and μ_2.

In addition, fifty broken pods whose defect dimension was equal or greater than 7 mm were selected at random. Each pod was weighed by an electronic balance (SARTORIUS S4100). All the sweet tamarind samples were uniformly mixed within cultivar and fed to the sorting system. The sweet tamarind was sorted out into four grades (small, medium, large, and defective). The feeding time and the number of correctly and incorrectly sorted pods in each receiver were recorded. Sorting efficiency E_w, mean contamination ratio $\bar{C}_R$ (error), and throughput capacity Q were evaluated as follows:

$$E_w = \sum\left(\frac{P_{gi}W_iG_i}{QP_i}\right) \quad (12)$$

$$W_i = \frac{K_iP_i}{\sum K_iP_i} \quad (13)$$

$$Q = \frac{W_t}{t} \quad (14)$$

$$\bar{C}_R = \frac{\sum N_{ij}}{\sum N_i} \quad (15)$$

where G_i is the outflow rate of grade i (pod/h); K_i is the fraction of cost as related to grade i; N_i is the number of grade i pods in the grade i receiver; N_{ij} is the number of grade j pods in the grade i receiver; P_i is the fraction of grade i pods of the total mixture at the beginning of sorting; P_{gi} is the fraction of correct pods in grade i receiver; Q is the inflow rate (pod/h); t is the feeding time (h); and W_t is the total pod weight fed into sorting system.

Referring to the samples of topic 2.3, thirty good pods of each cultivar were randomly chosen, mixed together, and manually fed into the sorting system for testing of shape separation. The number of correctly and incorrectly sorted pods in each receiver and feeding time were recorded.

3. Results and discussion

3.1. Camera height

The smallest error between the length of the predetermined square paper and that of the computer reading fell in the range of 2–4% for heights ranging from 40 to 44 cm. Accordingly, a height of 42 cm was set as optimum for the performance test.

3.2. Influence of belt speed, pod spacing, and orientation upon the parameters defining shape, size, and defects

The belt speed, the pod spacing, and orientation did not significantly affect the shape index and length of the sweet tamarind pods at a significance level of 5%. Table 1 provides the statistics of shape index as determined by Duncan multiple range test. The shape index of the curved, the slightly curved, and the straight pods were valued at 75.8, 61.6, and 51.1%, respectively. Straight, slightly curved, and curved pods possess sequentially higher shape indexes which agree with degree of curvature. The statistics of the lengths of the sweet tamarind pods with respect to size are given in Table 2. Three sizes (S, M, and L) were determined for both cultivars, with the range for Sitong pods extending from 10.1 to 14.0 cm, and 8.5 to 12.4 cm for Srichompoo pods. Sitong pods are larger than Srichompoo pods size by size. Sweet tamarind growers conventionally use length to visually size the pod. The belt speed, the pod spacing, and the orientation did not significantly influence defect detection at a significance level of 5%. Table 3 shows the percent of defects detected by the sorting system with regard to defect size. Detection ranged from 24.3% for 2-mm diameter holes to 90.8% for 13-mm diameter holes. This was because the larger defects were represented by more pixels in the image, and thus the image of larger defects was more clearly observed. This in turn gave rise to smaller differences between the true area and the read area and higher percent detection. The independence of shape, size, and defects with regard to variations in belt speed, pod spacing, and orientation suggests the development of an automatically fed sorting system.

Table 3
Detection rate of simulated defects on pod surfaces with respect to reference defect size

Diameter of simulated defect hole (mm)	Per cent detected
2	24.3 ± 4.3
3	68.0 ± 1.3
4	76.1 ± 2.9
5	81.6 ± 3.6
7	83.0 ± 2.0
10	87.9 ± 1.8
13	90.8 ± 1.4

3.3. Sorting system performance

Due to the non-influence of the belt speed, the pod spacing, and the orientation upon the variables of shape, size, and defects, the optimum operating conditions were determined to be a pod spacing of 25 cm and a belt speed of 13.34 mm/min (this speed was felt to best facilitate manual feeding). Table 4 shows that shape sorting efficiency under these conditions was recorded at 96.0%, with a mean contamination ratio of 4.0% and an average capacity of 1653 pod/h. Eq. (11) was applied to the associated samples of sweet tamarind to determine the length separation for the pod sizing test. "Medium" size for the Sitong and Srichompoo cultivars ranged from 11.4 to 12.8 cm and from 8.8 to 10.3 cm, respectively, (Table 5) with "small" and "large" size pods lying outside this range. The size separation in Table 5 complies with what was shown in Table 2. Table 6 presents the performance of the sorting system when it was tasked to separate good pods from defective pods of different sizes for a particular cultivar. The mean contamination ratio, sorting efficiency, and throughput capacity for Sitong pods of each size was 10.2%, 89.8%, and 1517 pod/h, respectively (5.7%, 94.3%, and 1,491 pod/h for Srichompoo). These ratios meet the requirements of the Thai agricultural commodities and food

Table 1
Shape index describing the sweet tamarind pods

Shape	Shape index
Curved	75.8 ± 6.5 a*
Slightly curved	61.6 ± 2.2 b
Straight	51.1 ± 1.2 c

* The same letter following the numbers in the same column implies insignificant difference of means at a significance level of 5%.

Table 2
Length of sweet tamarind pods analysed by Duncan multiple range test

Cultivar	Size	Length (cm)
Sitong	S	10.1 ± 0.47 a*
	M	12.0 ± 0.58 b
	L	14.0 ± 1.29 c
Srichompoo	S	8.5 ± 0.51 a
	M	10.0 ± 0.35 b
	L	12.4 ± 0.88 c

* The same letter following the number in the same column implied insignificant difference of means at a significance level of 5%.

Table 4
Sorting efficiency, mean contamination ratio, and average capacity of shape sorting

E_w (%)	$\bar{C}_R$ (%)	Q (pod/h)
96.0 ± 0.01	4.0 ± 0.01	1653 ± 74

Table 5
Estimated length separation for sweet tamarind sizing (cm)

Cultivar	Small, S	Medium, M	Large, L
Sitong	<11.4	11.4–12.8	>12.8
Srichompoo	<8.8	8.8–10.3	>10.3

Table 6
Performance of sorting system with respect to cultivar

Cultivar	Sorting efficiency E_w (%)	Mean contamination ratio, $\bar{C}_R$ (%)	Throughput capacity, Q (pod/h)
Sitong	89.8 ± 0.02	10.2 ± 0.02	1517 ± 57
Srichompoo	94.3 ± 0.02	5.7 ± 0.02	1491 ± 87

standards for export (Office of Thai Agricultural Commodity and Food Standard, 2003). The smaller $\bar{C}_R$ and higher E_w recorded for shape sorting than the combined $\bar{C}_R$ and E_w for size and defect sorting is perhaps because (a) the length of some pod samples distributed close to the range separation so that sorting was easily erroneous while the range of different shape index representing the pod shape was obviously isolated and (b) there are only three classes to be graded in shape sorting, while four classes (three sizes plus defects) are graded in combined sorting, which suggests that less contamination is likely to occur during shape sorting (see Eq. (15)). Another factor to note is that the smoother surface of Srichompoo pods causes the camera to accurately detect an image while with the rough surface of Sitong pods heightens the chance that the camera will sometimes detect shadows, which in turn will yield erroneous images. However, because the belt carrying the sweet tamarind pod was painted white, disturbance to the processed picture was minimized. Finally, system performance has been analyzed on the assumption that defects appear only on one side of the pod.

4. Conclusion

An image processing technique was developed to sort tamarind pods according to three qualities: shape, size, and defects. Software was written to characterize shape by shape indexes, size by image length, and defects by grey scale profile. The experimental machine vision sorting system was designed and constructed to test the software's ability to sort sweet tamarind pods when three control factors were varied. These factors were belt conveyor speed, pod spacing, and orientation. It was found that the control factors did not significantly affect the quality parameters. Optimum operating conditions were defined and the sorting system was tested to sort sweet tamarind according to shape, size, and defects. Evaluation showed that there were small errors in line with results reported in other experiments. Sorting performance was deemed to be acceptable in that it met Thai agricultural and food commodity standards.

References

Blasco, J., Aleixos, N., Molto, E., 2003. Machine vision system for automatic quality grading of fruit. Biosystems Engineering 85 (4), 415–423.

Chen, P., 1996. Quality evaluation technology for agricultural products. An Invited Paper presented in the International Conference of Agricultural Machinery Engineering, November 12–15, 1996, Seoul, Korea, pp. 11.

Gunasena, H.P., Hughes, M., 2000. Tamarind. International Center for Underutilized Crops, UK.

Jarimopas, B., Sirisawas, B., 2006. Transit damage and packaging of Thai sweet tamarind. In Proceeding of the Third National Technical Seminar on Post-harvest/Postproduction Technology, organized by the Postgraduate Education and Research Development Project in Post-harvest Technology, and Kasetsart University, 10–11 October 2005, Tipwiman Resort Hotel, Cha-am, Petchburee, Thailand, pp. 254–257.

Jarimopas, B., Sirisomboon, P., Sothornvit, R., Terdwongworakul, A., in press. The development of engineering technology to improve the production of tropical fresh produce in the developing countries. In: Pletney, Vivian N. (Ed.), Focus on Food Engineering Research and Development. Nova Science Publishers, Inc., New York.

Jarimopas, B., Nitasworakul, T., Lertchirapan, A., 1999. Evaluation of sizing quality of Thai madarin fruits. Thai Agricultural Research Journal 17 (3), 276–283.

Jayas, D.S., Karunakaran, C., 2005. Machine vision system in post-harvest technology. Stewart Post-harvest Review 2 (2), 1–9.

Kawano, S., 1994. Quality inspection of agricultural products by non-destructive techniques in Japan. Farming Japan 28 (1), 14–19.

Li, Q., Wang, M., Gu, W., 2002. Computer vision based system for apple surface defect detection. Computer and Electronics in Agriculture 36 (2002), 215–223.

Office of Thai Agricultural Commodity and Food Standard, 2003. Thai Agricultrual Commodity and Food Standard No. TACFS 5-2003: Mango. Ministry of Agriculture, pp. 6.

Pearson, T.C., Slaughter, D.C., 1996. Machine vision detection of early split pistachio nuts. Transaction of the ASAE 39 (3), 1203–1207.

Peleg, K., 1985. Produce Handling, Packaging and Distribution. AVI Publication Co., Inc., Connecticut. pp. 567.

Ruenfaikas, K., 2005. Measurement of sweet tamarind curvature. http://www.north.rit.ac.th/elecgmt2/tip/mkm.pd.

Sonka, M., Hlavac, V., Boyle, R., 1998. Image Processing, Analysis, and Machine Vision, second ed. PWS Publishing.

Serway, R.A., 1996. Physics for Scientists and Engineers with Modern Physics, fourth ed. Saunders College Publishing, Tokyo. pp. 1442.